

Active tendon control of suspension bridges: Study on the active cables configuration

Zhui Tian^{1,2a}, Bilal Mokrani^{*1}, David Alaluf^{1b}, Jun Jiang^{1c} and André Preumont^{1d}

¹Active Structures Laboratory, Université Libre de Bruxelles (ULB) 50, Av. F. D. Roosevelt (CP 165/42), Brussels, Belgium

²State Key Laboratory for Strength and Vibration of Mechanical Structures, Xi'an Jiaotong University, Xi'an 710049, China

(Received November 4, 2016, Revised February 7, 2017, Accepted February 24, 2017)

Abstract. In a previous study, the potential of damping suspension bridges with active stay cables has been evaluated on a numerical model of a suspension bridge, and demonstrated experimentally on a laboratory mockup. In this paper, we extend our study to explore two different configurations of the active stay-cables: one classical configuration, corresponding to attaching the active stay-cables between the top of the pylons and the deck (configuration I) and, another configuration, consisting of attaching the stay-cables between the base of the pylons and the catenary (configuration II). The analysis confirmed that both configurations are effective with a slight superiority of the second configuration. The study is conducted numerically and experimentally on a suspension bridge mock-up, by considering two types of active stay-cables. The experimental results confirmed the numerical predictions, and demonstrated the effectiveness of the second configuration.

Keywords: suspension bridge; active control; collocated control; integral force feedback

1. Introduction

Over the recent years, the improvement in construction materials and construction technology, computing capability, and above all a better understanding of the physics of the complex phenomena which control the external loads acting on structures, have revolutionized the civil engineering community, enabling the construction of large and elegant civil infrastructures, making the dreams of architects true. The natural damping of large civil structures tend to be small, and the dissipation of the vibration energy generated by the dynamic loadings is a central issue in the design.

Cable bridges are common civil structures exhibiting complex vibration problems and dynamic phenomena, such as wind and traffic induced vibration, flutter instabilities, and parametric excitations due to cable-structure interactions (Nayfeh and Mook 1979, Costa *et al.* 1996, Lilien and Costa 1994). As their size is continuously increasing, their resonance frequencies decrease and overlap with the frequency bandwidth of conventional

excitation loading such as pedestrians and joggers in footbridges. It is admitted that the over sensitivity to dynamic excitation of cable bridges is associated with the very low structural damping in the global bridge modes (often below 1%), and even less in the cable modes (Pacheco *et al.* 1993). A classical way to alleviate the vibrations in cable bridges is the use of damping systems, such as Tuned Mass Dampers TMD (Caetano *et al.* 2010, Tubino and Piccardo 2015, Bortoluzzi *et al.* 2015), viscous dampers for the cables (Tabatabai and Mehrabi, 2000), or active control using active tendons (Preumont, and Achkire 1997). Indeed, application of active tendons to flutter control was considered numerically by Yang and Giannopoulos (1979a,b) and experimental studies were pioneered by Fujino and co-workers (Warnitchai *et al.* 1993, Fujino *et al.* 1993, 1994). Since then, few studies considered this technique (Casciati *et al.* 2012).

This paper is concerned with active control techniques. It completes a previous study on the potential and the feasibility of active vibration damping of suspension bridges (Preumont *et al.* 2016). The study considers a suspension bridge supplemented with four active stay cables; the tension in the active cables is controlled by means of active tendons collocated with force sensors, and connected through decentralized Integral Force Feedback loops (Preumont *et al.* 1992). The study showed that it is possible to control suspension bridges with thin cables (of the same size as the hangers or even less), which do not need to withstand the dead load of the deck. In this paper, we extend our study to explore two possible configurations of the active cables. One configuration consists of connecting the cables between the top of the pylons and the deck, and another counter-intuitive configuration, connecting the cables between the catenary and the base of

*Corresponding author, Associate Professor

E-mail: bilal.mokrani@ulb.ac.be

^a Ph.D. candidate

E-mail: zhui.tian@ulb.ac.be

^b Ph.D.

E-mail: david.alaluf@ulb.ac.be

^c Ph.D.

E-mail: jun.jiang@mail.xjtu.edu.cn

^d Ph.D.

E-mail: andre.preumont@ulb.ac.be

the pylons, as suggested in (Auperin and Dumoulin 2001). The potential of Configuration II has been demonstrated numerically, by (Bossens 2001), on the model of the Askoy bridge, in Norway.

The present study is conducted numerically and experimentally on the suspension bridge mock-up, presented in (Preumont *et al.* 2016). The first part of the paper recalls the principles of the Integral Force Feedback strategy (IFF), as well as the design procedure for placing the active stay-cables. For the two configurations, we compare various possible locations of the active cables. Based on a simple formula, which predicts the maximum achievable damping with the IFF, we select the position providing the maximum damping for the targeted modes. In the second part of the paper, the two configurations are implemented on a laboratory suspension bridge mock-up. In this study, the cross section of the active cables is 4 times smaller than the bridge hangers.

2. Numerical analysis

The considered suspension bridge is represented in Fig.1. It has a span of 2.2 m and two articulated towers (pylons) of 0.62 m, the main steel cables (catenary) have a diameter of 1mm and the 2x10 hangers have a diameter of 0.5 mm; the deck is free to rotate at both ends and is attached to the catenary by the two rows of hangers.

2.1 Modelling

A linear model of the structure is used for the implementation of the various control configurations. The deck is modelled with finite elements of beams with bending stiffness and mass matching those of the experimental mockup, the main cables are modelled with bars (one element between two hangers) following a parabola (approximation of the catenary) and the hangers are also modelled with bars (a single element per hanger). The whole structure is analyzed in SAMCEF software and exported to Matlab for the implementation of the control system. The initial tensions in the hangers and the catenary are set to be symmetrical. Assuming a classical finite element formulation, the equation governing the dynamic response of the system is

$$M \ddot{x} + K x = -B T + f \quad (1)$$



Fig. 1 CAD view of the studied suspension bridge

where x is the vector of global coordinates of the finite element model, M and K are respectively the mass and stiffness matrices of the passive structure (including a linear model of the passive cables, if any, but excluding the active cables). The geometric stiffness due to the prestress is included in the model by applying a thermal field to the cables (Zhou *et al.* 2015). Note that the nonlinear dynamics, due to the nonlinear geometric effects, is ignored. The structural damping is neglected to simplify the presentation. The right hand side represents the external forces applied to the system; f is the vector of external disturbances such as gravity and wind loads (expressed in global coordinates), $T = (T_1, \dots, T_4)^T$ is the vector of tensions in the active cables and B is the influence matrix of the cable forces, projecting the cable forces in the global coordinate system (the columns of B contain the direction cosines of the various active cables); B depends on the topology of the active cable network.

2.2 Active control

The active control system consists of four active stay cables, attached either: (i) between the pylon and the deck, referred to as "Configuration I", Fig. 2(a); (ii) or between the main catenary and the pylon base, referred to as "Configuration II" Fig. 2(b). Each active tendon consists of a displacement actuator δ_i (e.g., piezoelectric) co-linear with a force sensor T_i . The displacements δ_i are controlled through decentralized Integral Force Feedback loops, such that

$$\delta_i = g s^{-1} k_i^{-1} T_i \quad (2)$$

where k_i is the stiffness of the i^{th} active tendon, and s is the Laplace variable. The theory of vibration control using Integral Force Feedback has been well established many years ago (Preumont *et al.* 1992), and confirmed experimentally on several occasions. In this section, we limit ourselves to recall the interesting formula predicting the maximum modal damping obtained with an IFF control system

$$\xi_i^{max} = \frac{\Omega_i - \omega_i}{2\omega_i} \quad (3)$$

where ω_i are the resonance frequencies of the structure excluding the active cables (obtained by considering the stiffness matrix K); and Ω_i are the resonance frequencies of the structure including the active cables stiffness (obtained by considering the stiffness matrix $K + BK_c B^T$, with

$$K_c = \text{diag}(k_i) \quad (4)$$

is the stiffness matrix of the cables); Eq.(3) was demonstrated in our previous paper (Preumont *et al.*, 2016). Based on Eq.(3), one can predict the maximum damping achievable with an IFF control, by simply performing two modal analyses of the structure: with and without the active cables.

Tables 1 and 2 show the maximum achievable damping for various possible positions of the active cables,

Table 1 Configuration I: Active control cables attached between the top of the pylon and the deck. Natural frequencies with (Ω_i) and without (ω_i) active cables and maximum achievable damping ratio ξ_i for the various modes and the various positions of the active cables shown in Fig. 2(a). (B-bending mode, T-torsional mode).

Mode #	Position A			Position B		Position C		Position D		Position E	
	ω_i (Hz)	Ω_i (Hz)	ξ_i^{\max} (%)								
1st B	5	6.5	15	8.1	31	7.9	29	6.1	11	5	0.0
2 nd B	6.8	6.8	0.0	6.8	0.0	7	1.5	7.6	6	7.6	6
1 st T	10.3	10.4	0.5	10.6	1.5	10.8	2.4	10.9	3	10.7	2
3rd B	11.4	13	7	14.2	12.3	12.4	4.4	11.4	0.0	11.7	1.3
2nd T	11.7	13.1	6	13.8	9	13.1	6	12.2	2.1	11.8	0.4
4 th B	17.8	19.8	5.6	19.3	4	17.6	0.6	18.2	1.1	17.7	0.3

Table 2 Configuration II: Active control cables attached between the catenary and the pylon base. Natural frequencies with (Ω_i) and without (ω_i) active cables and maximum achievable damping ratio ξ_i for the various modes and the various positions of the active cables shown in Fig. 2(b)

Mode #	Position A			Position B		Position C		Position D		Position E	
	ω_i (Hz)	Ω_i (Hz)	ξ_i^{\max} (%)								
1st B	5	6.7	17	9.1	41	9.4	44	7.37	24	5.9	9
2 nd B	6.8	6.8	0.0	6.8	0.0	6.9	0.7	7.3	3.7	7.3	3.7
1 st T	10.3	10.4	0.5	10.6	1.5	10.7	2	10.8	2.4	10.6	1.5
3rd B	11.4	13.2	8	15.2	16.7	13	7	11.5	0.4	11.4	0
2nd T	11.7	13.3	7	14.7	12.8	14.1	10	12.9	5	12.2	2
4 th B	17.8	20.2	6.7	20.5	7.6	17.6	0.6	17.9	0.3	17.6	0.6

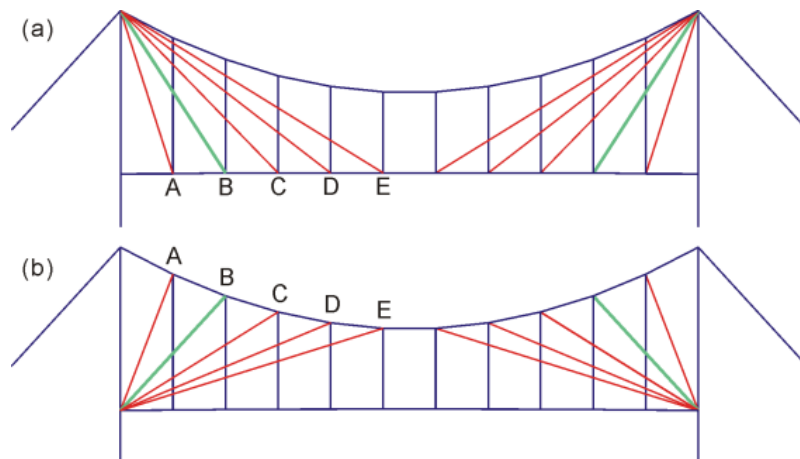
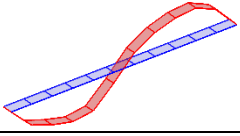
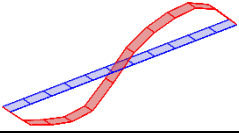
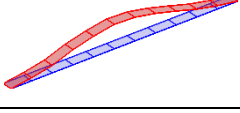
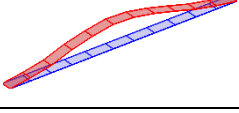
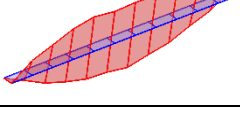
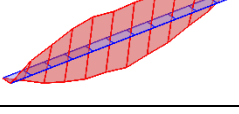
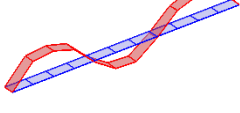
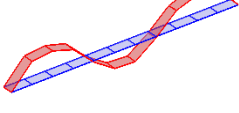
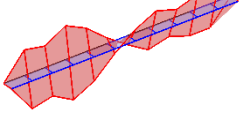
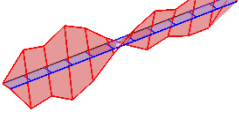
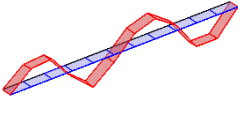
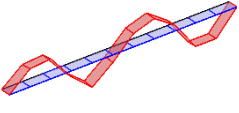


Fig. 2 Five possible positions for 4 symmetric active cables in two different configurations. (a) Configuration I: the active cables connect the pylons to the deck and (b) Configuration II: the active cables connect the base of the pylons to the catenary

corresponding respectively, to Configuration I of Fig. 2(a) and Configuration II of Fig. 2(b). The predicted values of damping are obtained from Eq. (3). For both configurations, Position B is an optimal for the 1st and the 3rd bending and 2nd torsional modes (which are in bold in the tables). Next we will consider position B for both configurations, I and II. Referring to Tables 1 and 2, one observes that both configurations, I and II, provide similar performances, with

a slight advantage for Configuration II. This advantage may be associated to the fact that configuration II relies on the absolute displacement of the catenary (as the second end of the active cables is clamped), while configuration I relies on the relative motion between the deck and the pylon. This advantage is also observed experimentally.

Table 3 Experimental results: comparison between Configuration I and II. Resonance frequencies, and corresponding mode shapes of the suspension bridge mock-up (only the deck is shown), without the active cables, and with the active cables mounted in position B (Configuration I and to Configuration II)

Mode	ω_i [Hz]	Mode shape without active cables	Conf. I Ω_i [Hz]	Conf. II Ω_i [Hz]	Mode shape with active cables
1 st B	5		9.1	9.4	
2 nd B	6		6	6	
1 st T	10.4		11	11	
3 rd B	11.5		14.3	15	
2 nd T	13.5		16.1	16.1	
4 th B	19.3		19.8	21	

3. Experimental Implementation

3.1 Setup

The experimental set-up is shown on Figs. 3 and 4. The catenary consists of a steel cable with a diameter of 1mm and the hangers are made of steel cables of 0.5 mm; the tension in the catenary and in the hangers can be adjusted with screws. The tension T_0 in a hanger is measured indirectly from its natural frequency f according to the string formula

$$f = \frac{1}{2L} \sqrt{\frac{T_0}{\rho A}} \quad (4)$$

f being measured by a non contact custom made laser sensor (Achkire and Preumont 1998). In this way, it was possible to distribute the tension in the hangers uniformly. Two types of active cables have been tested, one steel cable similar to the hangers, with a diameter of 0.5 mm, and one made of dyneema with a diameter of 0.2 mm; only the

results obtained with the dyneema cables are reported in this paper, since the results with steel cables have been already shown in our previous paper (Preumont *et al.* 2016).

We compare the two configurations shown in Fig. 2, with the active cables located at position B, for both configurations.

Fig. 4 shows a close view of the active tendon; it consists of a APA-50s piezoelectric actuator from CEDRAT with a stroke of 52 μm collocated with a B&K 8200 force sensor connected with a Nexus charge amplifier (the charge amplifier acts as a second-order high-pass filter with a corner frequency adjustable between 0.1 and 1 Hz). A small magnet is attached to the deck and a voice coil is used to apply a disturbance to the structure (band-limited white noise).

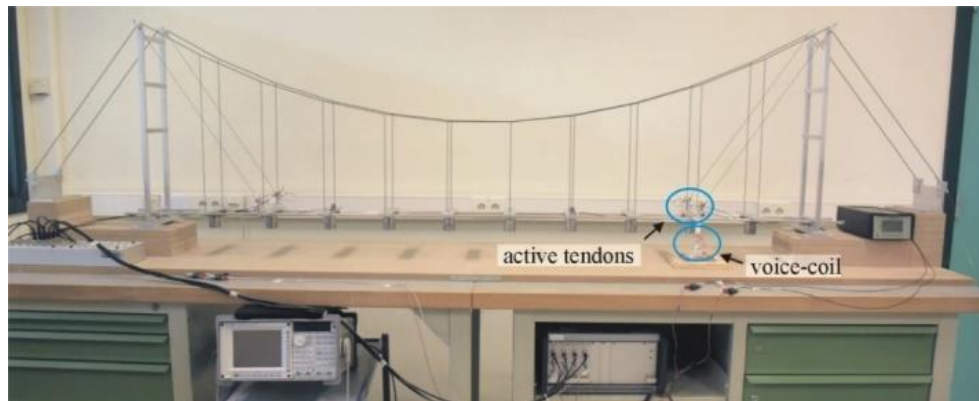


Fig. 3 Laboratory mock-up equipped with 4 active cables connecting the pylon to the deck (only Configuration I is shown)

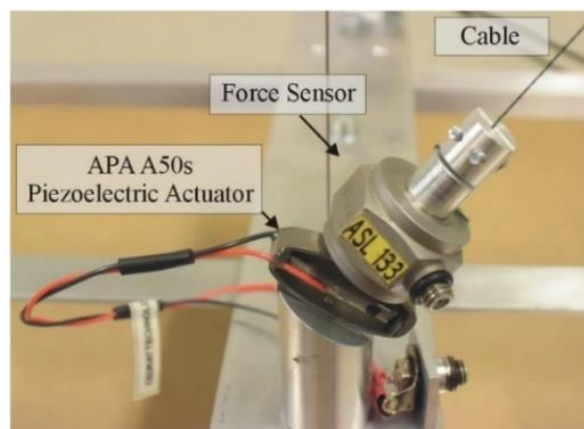


Fig. 4 Detail of the active tendon

3.2 Control

The critical aspects related to the modelling and the control system have been extensively discussed in our previous article (Preumont *et al.* 2016); we recall these aspects in the Appendix.

The effectiveness and the robustness of the IFF technique have been demonstrated on several occasions, and particularly on the suspension bridge mockup, numerically on a linear model, and experimentally on the laboratory mock-up. In our previous study, we considered active cables made of steel with 0.5 mm diameter (of the same size as the hangers). This has significant effect on the control performance, as the IFF technique relies on the amount of stiffness added by the active cables, as highlighted by Eq. (3). In this study, in order to demonstrate further the feasibility of the IFF control for real suspension bridges, we consider thinner Dyneema active cables of 0.2 mm diameter, with Young modulus similar to that of the steel cables. Recall that the goal of the current study is to compare one classical configuration (Configuration I, Fig. 2(a)), which is already used with passive stay cables and therefore more likely to be accepted by the civil engineering community, with a more exotic configuration (Configuration II, Fig. 2(b)), which has a slightly higher performance than the classical configuration

3.3 Results

Table 3 compares the resonance frequencies and their corresponding mode shapes of the suspension bridge without active cables, and with the active stay cables (no control) mounted according to Configuration I and to Configuration II (at position B, Fig. 2). Some changes in the order of the modes are observed: the first bending mode has the shape of the second mode of the bridge without active cables; the second mode has a shape similar to the first mode without active cables...etc. The mode shapes are almost unchanged for both configurations.

The active cables have a stiffening effect on almost all the modes, except on the second bending mode, on which the control system is not effective. Indeed, according to Eq. (3), the control system is more effective on the modes whose resonance frequencies deviation is large. The table compares the two configurations, and one can observe that Configuration II has a higher stiffening effect on the structure, and thus, a better control authority compared to Configuration I. This fact confirms the numerical predictions, depicted in Table 1 and Table 2.

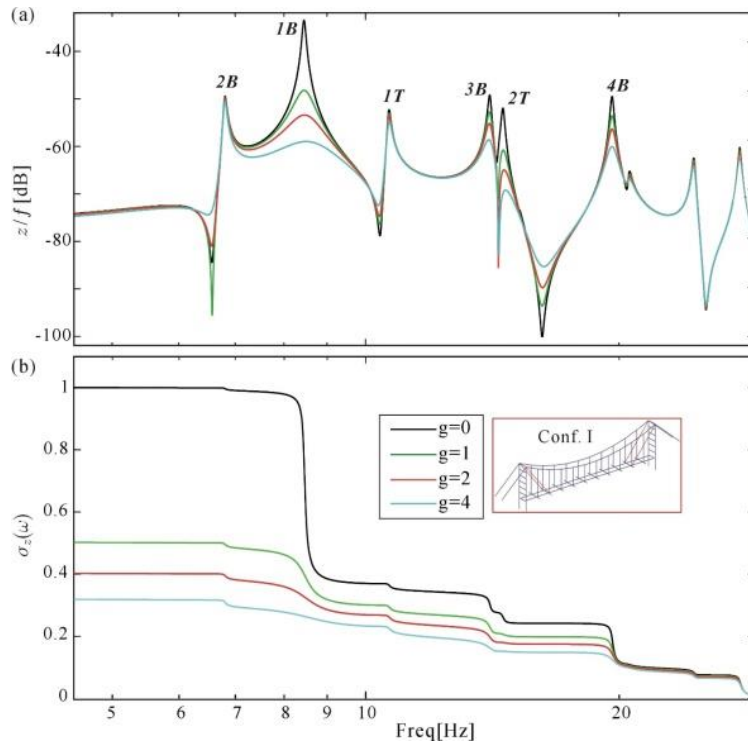


Fig. 5 Numerical results with Configuration I, for various values of the control gain g . (a) Numerical FRF z/f and (b) Corresponding cumulative RMS $\sigma(\omega)$, normalized to its value when $g = 0$

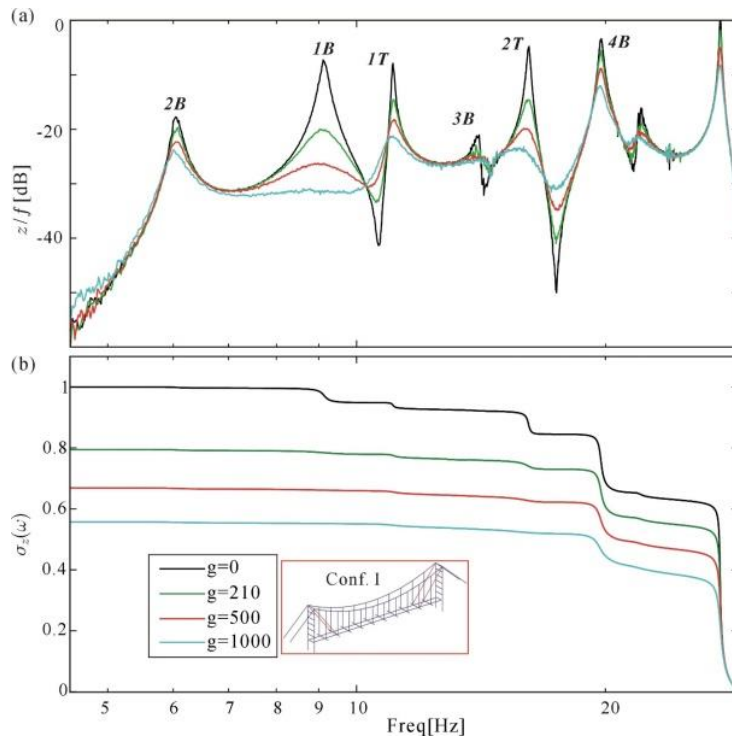


Fig. 6 Experimental results with Configuration I, for various values of the control gain g . (a) Experimental FRF z/f and (b) Corresponding cumulative RMS $\sigma(\omega)$, normalized to its value when $g = 0$

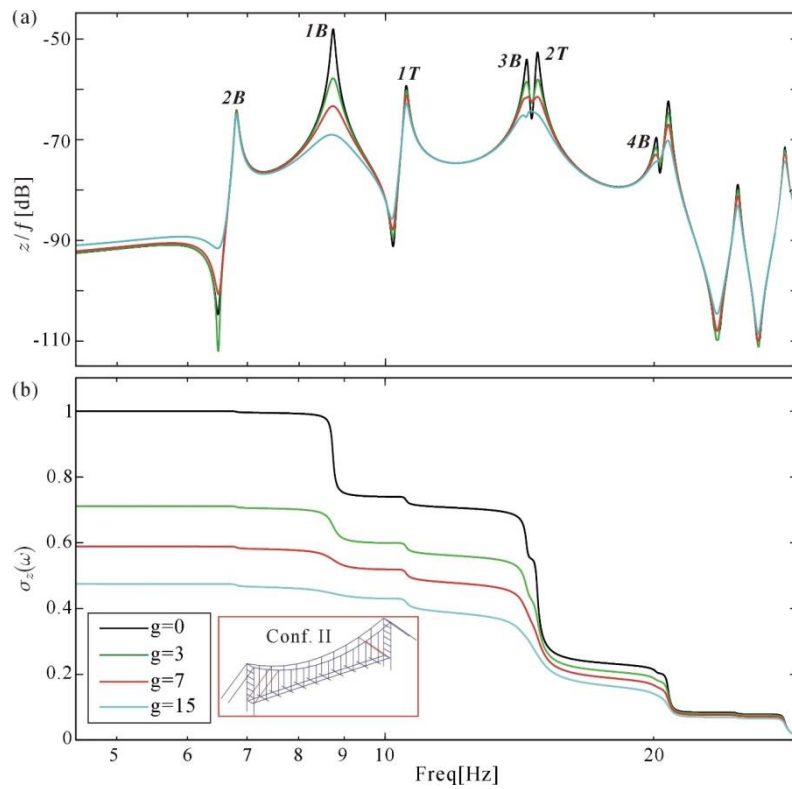


Fig. 7 Numerical results with Configuration II, for various values of the control gain g . (a) Numerical FRF z/f and (b) Corresponding cumulative RMS $\sigma(\omega)$, normalized to its value when $g = 0$

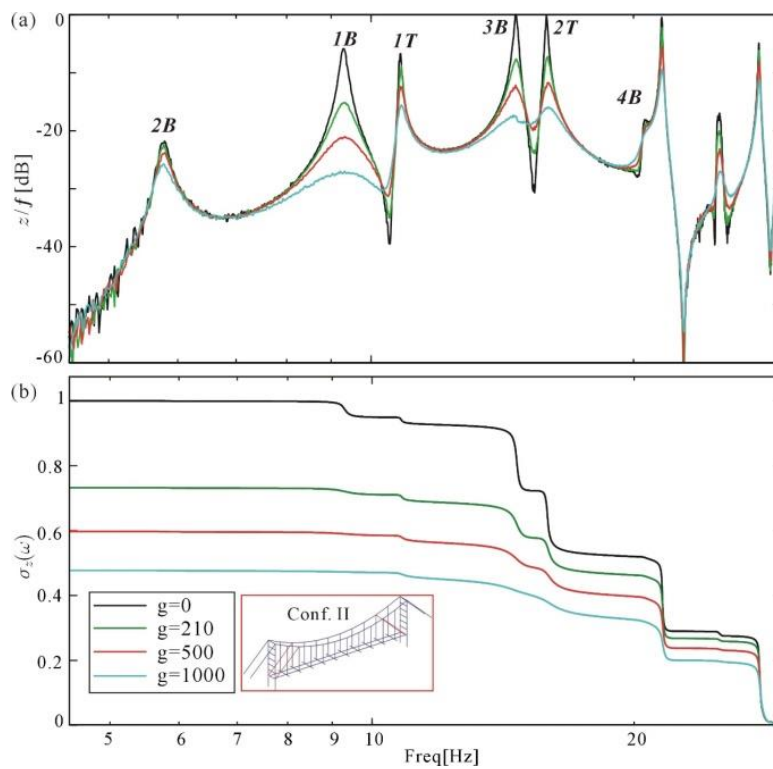


Fig. 8 Experimental results with Configuration II, for various values of the control gain g . (a) Experimental FRF z/f and (b) Corresponding cumulative RMS $\sigma(\omega)$, normalized to its value when $g = 0$

4. Conclusions

This paper completes a previous study on the feasibility of active damping of suspension bridges with the addition of stay cables controlled with active tendons. It extends the study to compare two configurations of the active stay cables: a classical configuration (Configuration I), where the active cables connect the top of the pylon to the deck, and a more exotic one (Configuration II), where the active cables connect the main catenary to the pylon base. The analysis and the numerical simulations show that both configurations prove effective, with a slight advantage to the second configuration, the experimental results confirm this fact. Moreover, the use of very thin Dyneema cables demonstrates, once again, the feasibility and the possibility of damping real suspension bridges, using a small number of thin cables, which do not need to withstand the weight of the deck.

Finally, from a dynamical point of view, considering the added stay cables without any control, this study demonstrates the stiffening ability of the second configuration, which appears to be counter-intuitive, compared to Configuration I, which is a classical configuration extensively used in classical and modern suspension bridges, to stiffen the deck.

Acknowledgments

The authors wish to thank Prof. Mihaita Horodincu from the Technical University "Gheorghe Asachi" Iasi, Romania, for his help in the construction of the bridge mock-up. Zhui Tian is supported by the China Scholarship Council (CSC, grant No. 201406280134). Bilal Mokrani is supported by the project Mecatec-M4, funded by "Région Wallone". The reviewers are gratefully acknowledged.

References

- Auperin, M. and Dumoulin, C. (2001), "Structural control: Point of view of a civil engineering company in the field of cable-supported structures", *Proceedings of the 3rd International Workshop on Structural Control, Paris 6-8 July 2000. Structural Control for Civil and Infrastructure Engineering*, (Eds., F. Casciati and G. Magonette), World Scientific Publishing, 2001.
- Achkire, Y., and Preumont, A. (1998), "Optical measurement of cable and string vibration", *J. Shock Vib.*, **5**, 171-179.
- Bortoluzzi, D., Casciati, S., Elia, L. And Faravelli, L. (2015), «Design of a TMD solution to mitigate wind-induced local vibrations in an existing timber footbridge», *Smart Struct. Syst.*, **16**(3), 459-478.
- Bossens, F. (2001), *Amortissement actif des structures câblées : de la théorie à l'implémentation*, PhD. Thesis, Université Libre de Bruxelles.
- Caetano, E., Cunha, Á., Moutinho, C. And Magalhães, F. (2010), "Studies for controlling human-induced vibration of the Pedro e Inês footbridge, Portugal. Part 2: Implementation of tuned mass dampers", *Eng. Struct.*, **32**(4), 1082-1091.
- Casciati, F., Rodellar, J. and Yildirim, U. (2012), "Active and semi-active control of structures—theory and applications: A review of recent advances", *J. Intel. Mat. Syst. Str.*,

1045389X12445029.

- Costa, A.P.D., Martins, J.A.C., Branco, F. and Lilien, J.L. (1996), "Oscillations of bridge stay cables induced by periodic motions of deck and/or towers". *J. Eng. Mech. - ASCE*, **122**(7), 613-622.
- Fujino, Y. and Susumpow, T. (1994), "An experimental study on active control of in-plane cable vibration by axial support motion". *Earthq. Eng. Struct. D*, **23**(12), 1283-1297.
- Fujino, Y., Warnitchai, P. and Pacheco, B.M. (1993), "Active stiffness control of cable vibration", *J. Appl. Mech.*, **60**(4), 948-953.
- Lilien, J.L. and Costa, A.P.D. (1994), "Vibration amplitudes caused by parametric excitation of cable stayed structures", *J. Sound Vib.*, **174**(1), 69-90.
- Nayfeh, A.H. and Mook, D.T. (1979), *Non Linear Oscillations*, Wiley, New York, NY, USA.
- Preumont, A., Dufour, J.P. and Malekian, C. (1992), "Active damping by a local force feedback with piezoelectric actuators", *J. Guid. Control Dynam.*, **15**(2), 390-395.
- Preumont, A. and Achkire, Y. (1997), "Active damping of structures with guy cables", *J. Guid. Control Dynam.*, **20**(2), 320-326.
- Preumont, A. (2011), *Vibration control of active structures: an introduction*, **179**, Springer Science and Business Media.
- Preumont, A., Voltan, M., Sangiovanni, A., Mokrani, B. and Alaluf, D. (2016), "Active tendon control of suspension bridges", *Smart Struct. Syst.*, **18**(1), 31-52.
- Tabatabai, H. and Mehrabi, A.B. (2000), "Design of mechanical viscous dampers for stay cables", *J. Bridge Eng.*, **5**(2), 114-123.
- Tubino, F. and Piccardo, G. (2015), "Tuned mass damper optimization for the mitigation of human-induced vibrations of pedestrian bridges", *Meccanica*, **50**(3), 809-824.
- Warnitchai, P., Fujino, Y., Pacheco, B.M. and Agret, R. (1993), "An experimental study on active tendon control of cable-stayed bridges", *Earthq. Eng. Struct. D.*, **22**(2), 93-111.
- Yang, J.N. and Giannopoulos, F. (1979a), "Active control and stability of cable-stayed bridge", *J. Eng. Mech. Division*, **105**(4), 677-694.
- Yang, J.N. and Giannopoulos, F. (1979b), "Active control of two-cable-stayed bridge", *J. Eng. Mech. Division*, **105**(5), 795-810.
- Zhou, Y., Sun, L. and Peng, Z. (2015), "Mechanisms of thermally induced deflection of a long-span cable-stayed bridge". *Smart Struct. Syst.*, **15**(3), 505-522.

FC

Appendix: Decentralized active damping of a cable-structure

Consider the cable-structure system similar to that of Fig. (A1), where a passive structure is connected to a set of active cables operated with active tendons. In the example shown, the passive structure consists of a vertical truss structure and there are 3 active cables and 3 active tendons. Each active tendon consists of a displacement actuator (e.g., piezoelectric) co-linear with a force sensor. T_i is the tension in the active cable i , measured by the sensor integrated in the active tendon, and δ_i is the free extension of the actuator, the variable used to control the system. k_i is the axial stiffness of the cable and the active tendon, jointly. We assume that the dynamics of the active cables can be neglected and that their interaction with the structure is restricted to the tension T_i . Assuming a classical finite element formulation, the equation governing the dynamic response of the system is:

$$M \ddot{x} + K x = -B T + f \quad (\text{A.1})$$

where x is the vector of global coordinates of the finite element model, M and K are respectively the mass and stiffness matrices of the passive structure (including a linear model of the passive cables, if any, but excluding the active cables); the structural damping is neglected to simplify the presentation. The right hand side represents the external forces applied to the system; f is the vector of external disturbances such as gravity and wind loads (expressed in global coordinates), $T = (T_1, \dots, T_i, \dots)^T$ is the vector of tension in the active cables and B is the influence matrix of the cable forces, projecting the cable forces in the global coordinate system (the columns of B contain the direction cosines of the various active cables); B depends on the topology of the active cable network.

If we neglect the cable dynamics, the active cables behave like (massless) bars. If $\delta = (\delta_1, \dots, \delta_i, \dots)^T$ is the vector of (free) active displacements of the active tendons acting along the cables, the tension in the cables are given by

$$T = K_c (B^T x - \delta) \quad (\text{A.2})$$

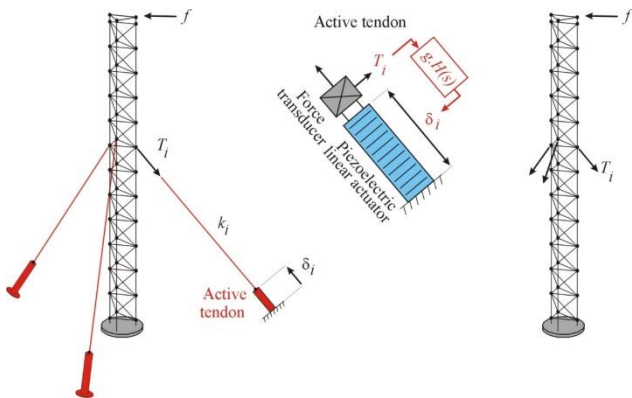


Fig. A.1 Left: Cable-structure system with active tendons. Center: Active tendon. Right: Passive structure

where $K_c = \text{diag}(k_i)$ is the stiffness matrix of the cables, $B^T x$ are the relative displacements of the end points of the cables projected along the chord lines. This equation expresses that the tension in the cable is associated with the elastic extension of the cable. Combining Eqs. (A.1) and (A.2), we get

$$M \ddot{x} + (K + BK_c B^T) x = BK_c \delta + f \quad (\text{A.3})$$

This equation indicates that $K + BK_c B^T$ is the stiffness matrix of the structure including all the guy cables (passive + active). Next, we assume that all the active cables are controlled according to the decentralized force feedback law

$$\delta = gh(s) \cdot K_c^{-1} T \quad (\text{A.4})$$

where $gh(s)$ is the scalar control law applied to all control channels¹ (note that $K_c^{-1} T$ represents the elastic extension of the active cables). Combining Eqs. (A.2)-(A.4), the closed-loop equation is

$$[Ms^2 + K + \frac{1}{1+gh(s)} \cdot BK_c B^T] x = f \quad (\text{A.5})$$

It is readily observed that the open-loop poles, solutions of the characteristic equation for $g = 0$, satisfy

$$[Ms^2 + K + BK_c B^T] x = 0 \quad (\text{A.6})$$

(the solutions are the eigenvalues of the structure with all cables), while the transmission zeros, solutions of Eq. (A.5) for $g \rightarrow \infty$, satisfy

$$[Ms^2 + K] x = 0 \quad (\text{A.7})$$

which is the eigenvalue problem for the open-loop structure where the active cables have been removed (they can be computed very easily).

Control law

If an Integral Force Feedback (IFF) controller is used, $h(s) = s^{-1}$, the closed-loop equation becomes

$$[Ms^2 + K + \frac{s}{s+g} BK_c B^T] x = f \quad (\text{A.8})$$

which indicates that the closed-loop static stiffness matrix is

$$\lim_{s \rightarrow 0} [Ms^2 + K + \frac{s}{s+g} BK_c B^T] = K \quad (\text{A.9})$$

This means that the active cables do not contribute to the static stiffness and this may be problematic in some applications. However, if the control is slightly changed into

$$gh(s) = \frac{gs}{(s+\beta)^2} \quad (\text{A.10})$$

where β is small and positive, the closed-loop equation becomes

¹ s is the Laplace variable.

$$[Ms^2 + K + \frac{(s+\beta)^2}{gs+(s+\beta)^2}BK_cB^T]x = f \quad (\text{A.11})$$

and the closed-loop static stiffness matrix becomes

$$\lim_{s=0} [Ms^2 + K + \frac{(s+\beta)^2}{gs+(s+\beta)^2}BK_cB^T] = K + BK_cB^T \quad (\text{A.12})$$

which indicates that the active cables have a full contribution to the static stiffness.

Modal Behavior

Next, let us project the characteristic equation on the normal modes of the structure with all the cables, $x = \Phi z$, which are normalized according to $\Phi^T M \Phi = 1$. According to the orthogonality condition of the normal modes

$$\Phi^T (K + BK_cB^T) \Phi = \Omega^2 = \text{diag}(\Omega_i^2) \quad (\text{A.13})$$

where Ω_i are the natural frequencies of the complete structure. In order to derive a simple and powerful result about the way each mode evolves with g , let us assume that the mode shapes are little changed by the active cables, so that we can write

$$\Phi^T K \Phi = \omega^2 = \text{diag}(\omega_i^2) \quad (\text{A.14})$$

where ω_i are the natural frequencies of the structure where the active cables have been removed. It follows that the *fraction of modal strain energy* is given by

$$\nu_i = \frac{\phi_i^T BK_cB^T \phi_i}{\phi_i^T (K + BK_cB^T) \phi_i} = \frac{\Omega_i^2 - \omega_i^2}{\Omega_i^2} \quad (\text{A.15})$$

Considering the IFF controller, the closed-loop characteristic Eq. (A.8) can be projected into modal coordinates, leading to

$$(s^2 + \Omega_i^2) - \frac{g}{g+s} (\Omega_i^2 - \omega_i^2) = 0$$

or

$$1 + g \frac{s^2 + \omega_i^2}{s(s^2 + \Omega_i^2)} = 0 \quad (\text{A.16})$$

This result indicates that the closed-loop poles can be predicted by performing two modal analyzes (Fig. A.3), one with all the cables, leading to the open-loop poles $\pm j\Omega_i$, and one with only the passive cables, leading to the open-loop zeros $\pm j\omega_i$, and drawing the independent root loci of Eq. (A.16). The maximum modal damping is given by

$$\xi_i^{\max} = \frac{\Omega_i - \omega_i}{2\omega_i} \quad (\text{A.17})$$

and it is achieved for $g = \Omega_i \sqrt{\Omega_i / \omega_i}$.

Eq. (A.17) relates directly the maximum achievable modal damping with the spacing between the pole Ω_i and the zero ω_i , which is essentially controlled by the fraction of modal strain energy in the active cables, as expressed by Eq. (A.15).

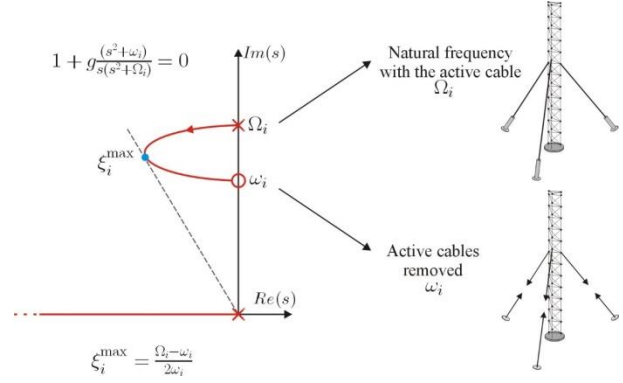


Fig. A.2 Root locus of the closed-loop poles with an IFF controller. The system is unconditionally stable